PAPER Special Issue on Optical Fibers and Devices

Development of Optical Isotropic E-Field Sensor Operating More than 10 GHz Using Mach-Zehnder Interferometers

Kimihiro TAJIMA[†a)], Ryuichi KOBAYASHI[††], Nobuo KUWABARA[†††], *and* Masamitsu TOKUDA[††††], *Regular Members*

SUMMARY An electric filed sensor using Mach-Zehnder interferometers has been designed to operate more than 10 GHz. The velocity of optical wave on the waveguide is investigated to determine the electrode length, and the characteristics of frequency response are analyzed using the moment method to determine the sensor element length. The electrode length of 1 mm and the element length of 8 mm are settled by these investigations. An isotropic electric field sensor is constructed using three sensors. The minimum detectable electric field strength is 22 mV/m at frequency bandwidth of 100 Hz. This is about 100 times for the conventional electric field sensor using the similar element. The sensitivity deviation is within 3 dB when temperature changes from 0 degree to 40 degree. The deviation of directivity can be tuned within ±1 dB to calibrate the sensitivity of the each element. The sensitivity degradation is within 6 dB up to 5 GHz and within 10 dB up to 10 GHz. This is almost agree with the calculated results. The sensor can measure almost the same waveform as the applied electric field pulse whose width is 6 ns and rise time is less than 2.5 ns.

key words: *EMC, electric field sensor, antenna measurement, optical modulator, electro-optical effect*

1. Introduction

The recent development of mobile multimedia communications has popularized the use of high frequency bands above 1 GHz in the new wireless services such as PHS (Personal Handy Phone System), PDC (Personal Digital Cellular Phone System), wireless LAN, Bluetooth and so on. These systems are sometimes used near electronic apparatus and cause electromagnetic compatibility (EMC) problems. Therefore, it is important to measure the electric field strength around mobile phone and radio communication equipment, and it is also important to evaluate the performance of EMC test equipment especially in frequency bands above 1 GHz. An electric field sensor using an optical modulator (optical E-field sensor) is suitable for this purpose because it has a wide bandwidth and small element.

On the other hand, the speed of CPU increases year by year and its clock frequency exceeds 1 GHz. This means we should consider electromagnetic compatibility (EMC) problems above 1 GHz because the interference might occur in these systems. The immunity and emission regulations of information technology equipment (ITE) above 1 GHz have been discussed at IEC/TC77 [1] and IEC/CISPR [2], [3] recently. The method to control electromagnetic environment above 1 GHz in the room under use of indoor wireless communication systems was also studied [4].

It is also important to measure the electric field strength and the electromagnetic pulse around information technology terminals above 1 GHz for studying EMC problem. However, conventional dipole antennas and horn antennas can not be used to these purpose because their size are too big to measure electric field near the equipment, and its frequency range is too narrow to measure the fast electromagnetic pulses. An Electric field sensor with short dipole elements was developed [5], but its sensitivity was not sufficient to measure electric filed distribution of mobile phone or ITE, moreover, its frequency range was not broad to measure electromagnetic pulses.

In order to solve these problems, electric field sensors using optical modulators (optical E-field sensors) have been developed [6]–[11]. However, there are still some defects in these conventional optical E-field sensors. One of them is the frequency range degradation over GHz band.

The optical E-field sensor with element length of 210 mm could detect 0.1 mV/m [6]. However, the frequency range was limited up to 1 GHz in the most of optical E-field sensors [6]–[10] because of the sensor element resonance. The optical E-field sensor with very short sensor element (10 mm) has been developed [11]. Although it was expected for the sensor to operate more than 10 GHz considering resonance frequency of sensor element, in fact the frequency range was limited to less than 4 GHz caused by the influence of the dielectric material as the sensor case on the electromagnetic wave velocity [11].

In this paper, we develop an optical isotropic E-field sensor operating up to more than 10 GHz. First, we fabricate the sensors whose element length are determined by considering the dielectric constant of the sensor case [11] and investigate whether the material of the sensor case would limit the frequency range. Secondly, the new design method is studied to consider the transit time effect of the optical wave. The thirdly, an isotropic optical sensor is fabricated using the new design method and characteristics of the sensor are measured.

Manuscript received August 20, 2001.
Manuscript revised October 26, 2001.

† The authors is with NTT Service Integration Laboratories, Musashino-shi, 180-8585 Japan.
†† The author is with NTT Technical Assistance and Support Center, Musashino-shi, 180-8585 Japan.
††† The author is with Kyushu Institute of Technology, Kitakyusyu-shi, 804-8550 Japan.
†††† The author is with Musashi Institute of Technology, Tokyo, 158-8557 Japan.
a) E-mail: tajima.kimihiro@lab.ntt.co.jp

2. Frequency Response of Optical E-Field Sensor with Short Sensor Element

The structure of an optical E-field sensor with very small elements is illustrated in Fig. 1. This sensor consist of a set of an optical sources, a polarization-maintaining fiber, a Mach-Zehnder interferometer with a dipole element, a single-mode fiber, a photodetector and a level meter. Two metallic elements are aligned on an optical modulator as forming a dipole antenna. When an electric field is applied to the sensor element, a voltage is induced across the gap between electrodes on the modulator. The modulator converts this voltage into an optical signal in proportion to the electric field strength. The amplitude of the optical signal is measured using a photodetector and a level meter. A laser diode or high-power Nb:YAG laser pumped by a laser diode is used as the optical source, and a photodiode, such as a PIN photodiode or APD (Averavche photodiode), is used as the photo-detector.

In order to minimize the influence of the sensing part against the electromagnetic field to be measured, every part and section of the sensor consists of nonmetallic materials except sensor elements and electrodes. The sensor case including an optical modulator is made of ceramic composite having less thermal expansion coefficient.

The bandwidth of an optical E-field sensor can be expanded by reducing the length of sensor element. The relationship between frequency bandwidth and element length has been studied in a paper [11]. Using a taper-patterned nichrome film deposited on a glass substrate, a travelling wave dipole antenna with resistance can be formed. In such device, it is possible to make resonance suppressed and frequency characteristic broad over 1 GHz.

The equivalent circuit of the sensor is shown in Fig. 2, for analyzing theoretically the sensitivity and frequency characteristics. The output voltage of photodetector V_{out} is given by Eq. (1).

$$V_{out} = \eta_d P_{out}, \tag{1}$$

where

$$P_{out} = \eta_s \eta_m \eta_p P_{in} \{1+\cos(\phi_1 - \phi_2 - 2\Delta\phi)\}/2 \tag{2}$$

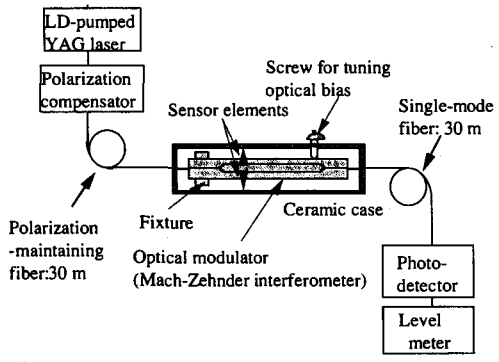

Fig. 1 Configration of the electric-field sensor with very short elements using Mach-Zehnder interferometer.

$$\phi_m = \phi_1 - \phi_2, \tag{3}$$

$$2\Delta\phi = \pi V_c / V_\pi, \tag{4}$$

$$V_c = Z_m / (Z_a + Z_l + Z_m)\, E\, h_e. \tag{5}$$

Here, η_d is the conversion constant of the photodetector, P_{in} is the optical input power to the optical fiber connected to the modulator, P_{out} is the optical output power from the optical fiber connected to the modulator, η_p and η_s are the transmission loss constants of the optical fibers connected to the input and output port of the modulator, η_m is the insertion loss constant of the modulator, ϕ_1 and ϕ_2 are the phase changes of optical waves in each waveguide, ϕ_m is the optical bias angle which is a phase deviation between two waveguides in Mach-Zehnder interferometer. V_c is the voltage at the input terminal of the modulator induced by the applied electric field, V_π is the half-wave voltage of the modulator, Z_a is the driving point impedance of the sensor elements, E is the applied electric field strength, h_e is the effective length of the sensor element, Z_l is the loaded impedance with the sensor element and Z_m is the input impedance of the optical modulator. Z_a, h_e, and Z_l are calculated using the moment method.

Two optical E-field sensors, whose element length h are 8 mm and 10 mm and both electrode length are 2 mm, have been fabricated and those frequency responses were measured. The results are shown in Fig. 3. In this figure, the horizontal axis is for the frequency, and the vertical axis is for the relative output voltage normalized by the values at 1 GHz. The black solid lines show the values of h = 10 mm and the

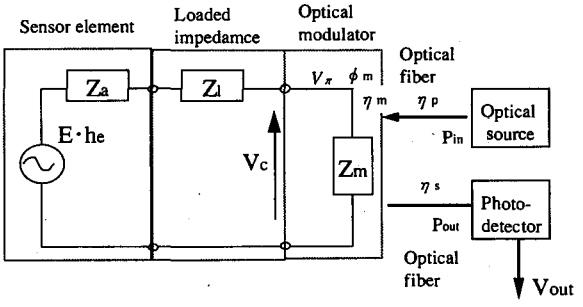

Fig. 2 Equivalent circuit of electric field sensor.

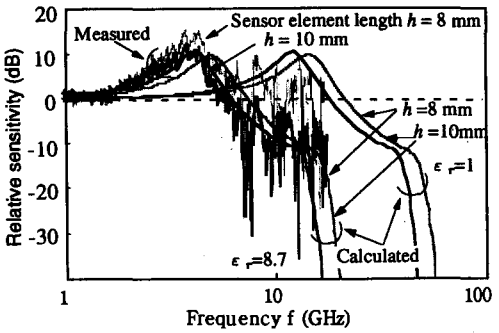

Fig. 3 Frequency bandwidth degradation of optical E-field sensor.

gray solid lines show the values of h = 8 mm, and the measured results and the results calculated by the moment method are compared.

In the paper [11], we determined the sensor element length by considering the influence of sensor case material. We presumed that the dielectric constant of the case material would limit the frequency bandwidth. As shown in Fig. 3, this assumption would be correct, however, it was found that there were no changes in frequency responses between with the sensor case and without it. This means that the frequency response of this optical E-field sensor is not influenced too much by sensor case materials, such as the ceramic (ε_r = 8.7). If the cause of degradation in frequency range can be solve, it is expected that the frequency range of the sensor must be expanded extremely with shortening sensor element, h = 10 mm, 8 mm, as shown in case of ε_r = 1 of Fig. 3.

Therefore, the new design method should be studied for the realization of optical E-field sensor with broad bandwidth operating more than 10 GHz.

3. Analysis of the Frequency Characteristic Considering Transit Time Effect

A really fabricated sensor has degradations in frequency range not relating to element length. Without those degradations, it is expected that the bandwidth would be more than 10 GHz with element length h = 10 mm. It is considered that one reason of this degradations is the influence of mismatching between the velocity of light wave in optical waveguides and the velocity of electromagnetic wave on electrode of Mach-Zehnder interferometer. Thus it is important to analyze the relationship between the frequency response and the configuration of the sensor.

The analysis model of sensor element and electrode on optical modulator can be presented as shown in Fig. 4. As the mismatching phenomenon for velocities, transit time effect of traveling-wave in the optical modulator is known well [12], [13]. This is the influence of mismatching between the velocity of light wave and the velocity of electromagnetic wave on modulation. Originally, since the optical modulator of this type E-field sensor is regarded as the lumped electrode type and it has been simply presented by a capacitance as shown in Fig. 2 [12], it is usually considered that transit time effect of traveling-wave does not occur. However, strictly speaking, the point that the electrodes of this modulator are not resistively terminated is remarkably different from the typical type of lumped optical modulator. In this section, we analyze numerically the frequency characteristic by considering the transit time effect.

Figure 5 shows the illustration explaining a transit time effect. The vertical axis shows the induced voltage at the electrodes $V(t)$ and the horizontal axis shows the transit time of light wave in waveguide of $LiNbO_3$. We can not neglect the electrode length against the electromagnetic wave length over several GHz band. The induced voltage at the electrodes $V(t)$ varies between $V(0)$ and $V(t_0)$ when the transit time t_0 become close to the period time of electromagnetic wave t_f.

From Eq.(2), when ϕ_m is $\pi/2$, the modulation component P_m is given by

$$P_m = K_m\{\sin(2\Delta\phi)\} \tag{6}$$

where

$$K_m = \eta_s\eta_m\eta_p P_{in}/2 \tag{7}$$

when $\Delta\phi \ll 1$, then

$$P_m = K_m \cdot 2\Delta\phi \tag{8}$$

The transit time of the optical wave t_0 is given by

$$t_0 = l_0/v_0 = l_0 n_e/c \tag{9}$$

where l_0 is the electrode length, v_0 is the velocity of optical wave in waveguide (= c/n_e), c is the velocity of light wave in free space (= 2.998×10^8 (m/sec)), n_e is the refractive index of the waveguide. The period time of the detected electric field signal is given by

$$t_f = 1/f \tag{10}$$

where f is the frequency of the detected electric field signal.

When $t_0 \ll t_f$, $\Delta\phi$ is presented by Eq. (4) and when t_0 is close to t_f, $\Delta\phi$ is presented by the function of t_0. When we consider sub-segment Δl, the transit time Δt is given by

$$\Delta t = \Delta l/v_0 = \Delta l\, n_e/c \tag{11}$$

Since $\Delta t \ll t_f$, P_m is given by the sum of $\Delta\phi$ at the each position Δl of electrode as follows,

$$P_m = 2K_m\{\Delta\phi(0)\cdot(\Delta l_0/l_0) + \Delta\phi(\Delta t)\cdot(\Delta l_1/l_0) + \Delta\phi(2\Delta t)\cdot(\Delta l_2/l_0) + \cdots + \Delta\phi(n\Delta t)\cdot(\Delta l_n/l_0) + \cdots$$

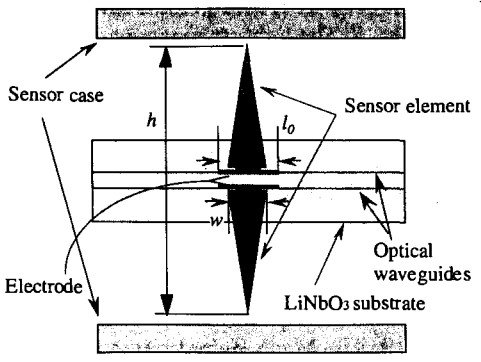

Fig. 4 Analysis model of sensor element and electrode.

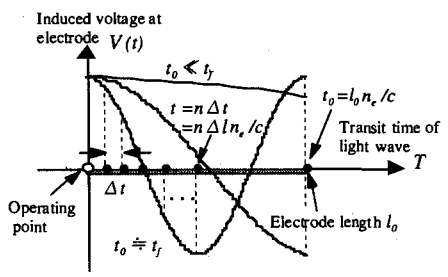

Fig. 5 Image of transit time effect on lumped modulator.

$$+\Delta\phi(N\Delta t)\cdot(\Delta l_N/l_0)\} \quad (12)$$

where

$$N = l_0/\Delta l = t_0/\Delta t. \quad (13)$$

Now, we present V_c in Eq. (4) as Eq. (14)

$$V(t) = V_c\cos(\omega t+\theta) \quad (14)$$

where

$$t = n\Delta t = n\,\Delta l/v_0 = n\,\Delta l\, n_e/c. \quad (n=1, 2, 3\cdots N) \quad (15)$$

Substituting Eq. (4), Eq. (14) and Eq. (15) for Eq. (12), then we get

$$\begin{aligned} P_m &= 2K_m\sum_{n=1}^{N}[\{\pi V_c\cos(\omega n\Delta l/v_0+\theta)/V_\pi\}(\Delta l_n/l_0)] \\ &= 2K_m\{\pi V_c/(V_\pi l_0)\}\sum_{n=1}^{N}\{\cos(\omega n\Delta l/v_0+\theta)\Delta l_n\} \\ &= 2K_m\{\pi V_c/(V_\pi l_0)\}\int_0^{l_0}\cos(\omega l_0/v_0+\theta)\,dl \\ &= 2K_m\{\pi V_c/(V_\pi l_0)\}(v_0/\omega)\cos\{\omega l_0/(2v_0)+\theta\} \\ &\quad\cdot\sin\{\omega l_0/(2v_0)\} \end{aligned} \quad (16)$$

Then, we get

$$P_m = K_m(\pi V_c/V_\pi)\cos\{\omega l_0/(2v_0)+\theta\}\frac{\sin(\omega l_0/v_0)}{\omega l_0/v_0} \quad (17)$$

When $t_0 << t_f$, and $\theta = 0$, we get

$$\omega l_0/(2v_0) = \pi(t_0/t_f) << 1 \quad (18)$$

Then Eq. (17) become

$$P_m = K_m(\pi V_c/V_p). \quad (19)$$

Equation (19) agrees with Eq. (7).

Figure 6 shows the frequency characteristics of sensitivity calculated by Eq. (1) using the output power expressed by Eq. (17). The vertical axis shows the relative sensitivity normalized by the value of sensitivity at 100 Hz. In this calculation, we used parameters listed in Table 1 and the electrode length l_0 was varied in 1, 2, 5, 10, 40 mm respectively. The element length h was 8 mm, element width w was 0.5 mm and the input impedance of the optical modulator Z_m which was expressed by the parallel connection of a resistance R_m: 14 MΩ and a capacitance C_m: 1 pF. Both of the driving point impedance Z_a and the effective length h_e of the sensor element were solved using the moment method which was applied to sensor element considered as a dipole antenna. The value of resistively loaded impedance with the sensor element Z_l was calculated in a same way as [14]. The distribution of loaded resistance was improved against the resonant phenomenon around 4.5 GHz in Fig. 3. The amplitude of voltage induced by applied electric field strength V_c was set to 1 V and the phase angle θ was set to 0.

It is shown that the frequency bandwidth of this optical E-field sensor is restricted by the electrode length in spite of very short sensor element. This calculation result agrees well with the experimental fact in Fig. 3 that the frequency bandwidth would not be broad as shortening the sensor element.

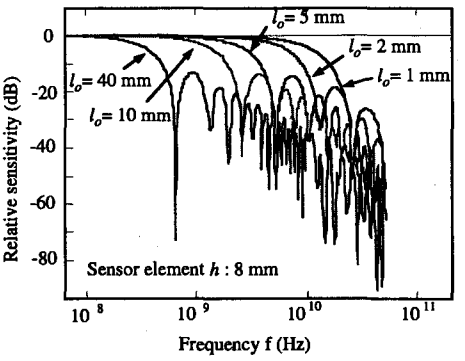

Fig. 6 Calculated frequency response of optical E-field sensor when the electrode length is changed.

Table 1 Calculation parameters for estimation of frequency characteristics.

Element width w	0.5 mm
Element length h	8 mm
Optical bias angle ϕ_m	1.57 rad
Refractive index n_e	2.14
Phase angle θ	0 rad
Half-wave voltage V_π	2.0 V
Resistance of Si buffer R_m	14 MΩ
Capacitance of modulator C_m	1 pF
Optical input power p_{in}	30mW
Insertion loss constant of the modulator η_m	0.25
Transmission loss constants of optical fibers η_p, η_s	1.0
Conversion constant of photo-detector η_d	250 V/W

4. Measured Characteristics

The improved broad-band optical E-field sensor has been fabricated as an isotropic sensor as shown in Figs. 7 and 8, and its characteristics were measured. Isotropic sensor is useful to evaluate the electric field strength near the electronic equipment and the electromagnetic pulse because polarizations of electromagnetic waves are not always uniform in real environments, like electrostatic discharge and the near field around a cellular phone [15]. The configuration of the new sensor is illustrated in Fig. 8. The light source was a LD-pumped YAG laser with a wavelength of 1.3 μm and an output power of 30 mW (14.8 dBm). The photodetector was a PIN photodiode (HP11982) with a frequency range of DC to 15 GHz. The Level meter was a spectrum analyzer (HP8562A) with a frequency range of 100 kHz to 22 GHz and with setting a video band width of 100 Hz, a frequency span of 0 Hz and a sweeptime of 500 ms.

The sensing part consists of three Mach-Zehnder interferometers mounted on each surface of a triangular pole as shown in Fig. 9. The Mach-Zehnder interferometers had a half-wave voltage of less than 2 V and an operating band-

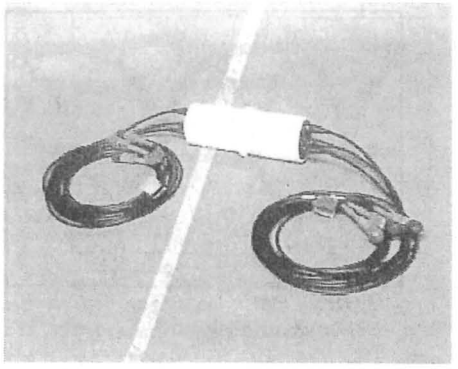

Fig. 7 Photograph of a fabricated isotropic E-field sensor using optical modulator.

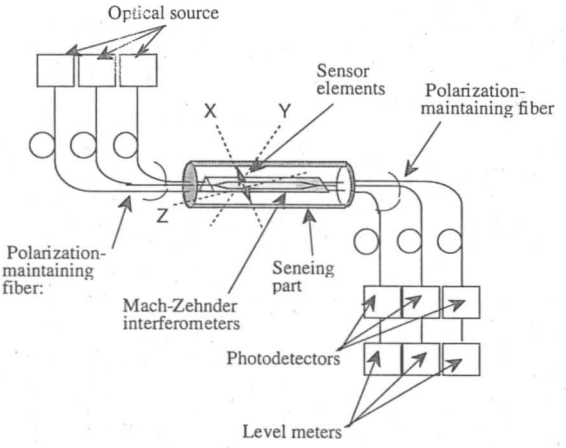

Fig. 8 Configuration of the optical isotropic E-field sensor using Mach-Zehnder interferometer.

width ranging from DC to more than 10 GHz. It was formed by Ti diffusion on a 55-mm-long, 1-mm-wide, 0.5-mm-thick, Z-cut $LiNbO_3$ substrate. The waveguides, which were divided into two path, were 40-mm-long, and the separation between them was 26 μm. The insertion loss of the optical modulator was less than 11 dB, and the optical bias angle was tuned to 1.57 radian by tuning a screw located on the side of the sensor case.

Its outside case, whose size is 128 mm long and 44 mm in diameter, is made of Teflon. The triangular pole is made of Noryl which is one of the Polyphenyleneoxide material and whose coefficient of linear therm is quite small. Each of the sensor elements, which is an 8-mm-long dipole antenna, consists of two pieces of 0.5-mm thick glass plate with a 150-Å thick tapered (0.5 mm at the base, 4 mm high) nichrome film. Each element is attached to each optical modulator at an angle of 54.7° with respect to the optical waveguide. If the three elements on modulators are gathered at the center point of the triangular pole, those cross at right angles and form an imaginary isotropic antenna as shown in Fig. 9.

This structure is well known in [15] as the conventional isotropic E-field sensor without optical modulators and fibers. The parameters for sensor element are shown in Table 2.

Table 2 Parameters for sensor element of a new fabricated optical E-field sensor.

Element length h	8 mm
Element width w (the base)	0.5 mm
Element thickness t	150 Å
Electrode length l_0	1 mm
Angle of element with substrate ρ	54.7°

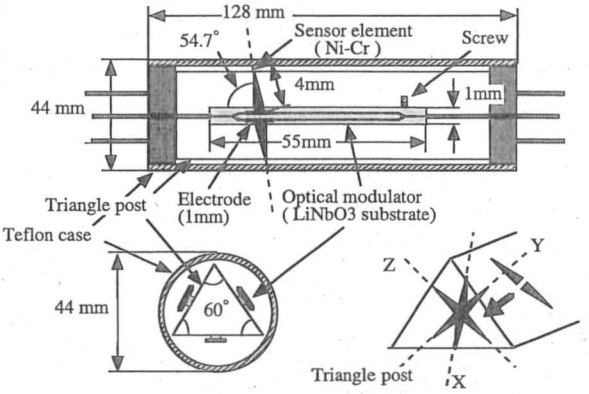

Fig. 9 Structure of the sensing part of fabricated E-field sensor.

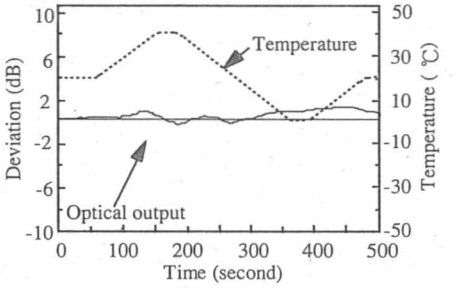

Fig. 10 Optical output power deviation with changing temperature.

The element length 8-mm-long and the electrode length 1-mm-long were decided by referring to the calculation result in Fig. 6 in order to achieve the frequency deviation of less than 4 dB at 10 GHz.

Because the structure of this new sensor is very complicated, it is important to evaluate its temperature characteristic. The sensor was placed in a chamber and the temperature in the chamber was varied from 0 to 40°C during a 500-minute cycle. The optical output power of the modulator was measured with an optical power meter. The measured result is shown in Fig. 10. The deviations of optical output level were almost within 3 dB and it is confirmed that the temperature characteristic of this new sensor is quite stable.

The sensitivity characteristics are shown in Fig. 11. The output voltages of the optical detector were measured at 1.5, 1.9, and 2.5 GHz under various applied electric field strengths in the GTEM cell, where the electric field strength was varied from 84 to 158 dB (μV/m) (measurement limit). The results at three frequencies were close to each other. The dynamic range was over 70 dB, the antenna factor was 87 dB,

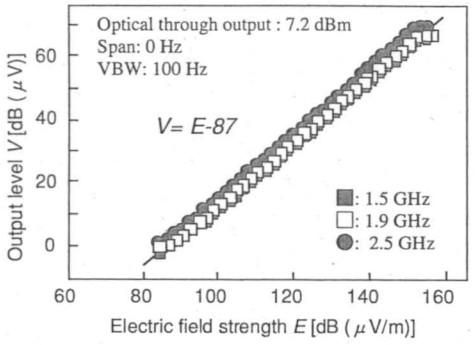

Fig. 11 Sensitivity characteristics of isotropic optical E-field sensor.

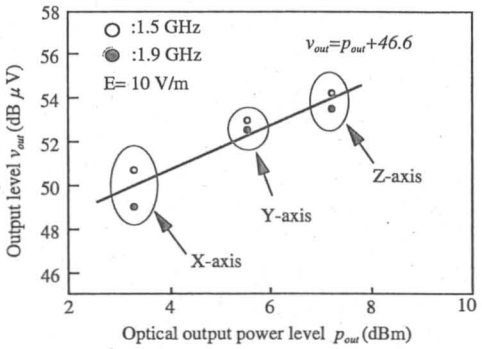

Fig. 12 Sensitivity comparison between the each *X*, *Y* and *Z*-axis Mach-Zehnder interferometer.

and the minimum detectable electric field strength was 87 dB(μV/m) (= 22 mV/m). The sensitivity obtained by a commercial E-field sensor, having an element almost the same size, was 2 V/m, indicating that our sensor is 100 times more sensitive.

Figure 12 shows the sensitivity comparison between the each *X*-axis, *Y*-axis and *Z*-axis Mach-Zehnder interferometer. The insertion loss of each modulator was different and those were about 6–11 dB. As shown in Fig. 12 and Eq. (1), the output level of photodetector increases in proportion to the optical output level of interferometer. In the real measurement, a calibration of optical output level between each optical modulator should be needed to make the standard levels of three modulators uniform.

The directional characteristics were measured in a semi-anechoic chamber with 30-cm-thick RF absorbers on its conductive ground plane. A horizontally polarized wave was applied from a horn antenna 3 m away from the sensor, whose *X*-axis element was placed in the vertical direction and the turn-table was rotated every 15° (total rotation of 360°). Figure 13 shows the directional pattern of the sensor. The output voltages was measured for the *X*-axis (□), the *Y*-axis (●) and the *Z*-axis (○) respectively. In this figure the vertical axis is the relative output voltage, and the maximum value of the *Y*-axis was used for reference (0 dB). The total electric field strength of the three directions is given by

$$E_{total} = \sqrt{E_x^2 + E_y^2 + E_z^2} \tag{7}$$

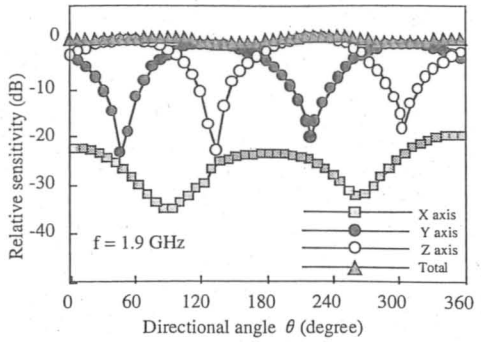

(a) *X*-axis element is vertical, the horizontal plane wave against *Y* and *Z* axis element.

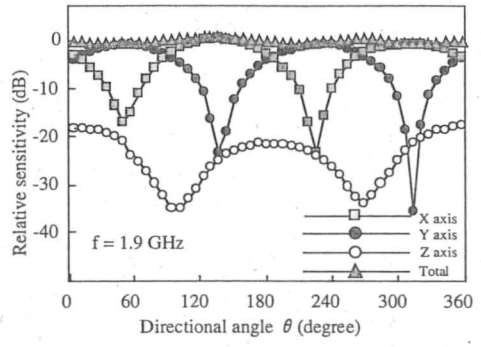

(b) *Z*-axis element is vertical, the horizontal plane wave against *X* and *Y* axis element.

Fig. 13 Directional pattern of isotropic optical E-field sensor in the plane including sensor element.

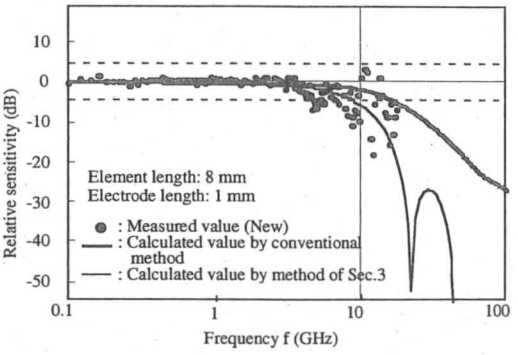

Fig. 14 Measured frequency response of fabricated isotropic optical E-field sensor.

where E_x, E_y, and E_z are the components of the electric field strength along the *X*, *Y*, *Z*-axis respectively.

The measured results in Fig. 13 show that the directional characteristics of the total electric field were almost isotopic and the deviations of sensitivity were within ±1 dB for any direction. The pattern of each element was similar to that of a tuned dipole antenna.

The measured frequency characteristics are shown in Fig. 14. The black circles (●) shows the measured values of this new isotropic optical E-field sensor, the gray solid line shows the calculated values by the moment method with-

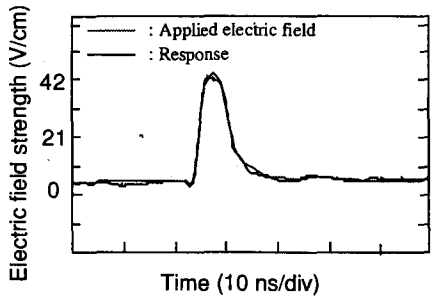

Fig. 15 Response for applying nano-second impulse.

out considering transit time effect of electrode and the black solid line shows the one considering transit time effect. In this figure, the horizontal axis is for the frequency value, 100 MHz to 100 GHz, and the vertical axis shows the relative output voltage normalized by the values at 100 MHz. The measurement was done in the GTEM cell, whose electric field strength was calibrated using an electric field probe (EMCO Model 7121). It is shown that the sensitivity of the sensor was relatively constant within –10 dB at frequencies from 100 MHz to 10 GHz.

The calculated values without considering the transit effect indicate that the sensor can operate over than 10 GHz but it does not agree with the measurement results. On the other hand, the calculated values considering with the transit effect agree well to measure results. This means the transit time effect should be considered to design the electric filed sensor operating above several GHz. The calculated values agree well to measured values. In this new sensor, the resonant phenomenon were improved by optimizing resistive elements [14].

This sensor must be useful for measuring electromagnetic pulses, for instance, generated by electrostatic discharge. In order to evaluated broad bandwidth characteristic of this new sensor, we measured fast impulses. An example is shown in Fig.15. A 6-ns-width (full width at half maximum) impulse whose rise time is about 2.5 ns was measured by this new sensor in a TEM cell whose bandwidth was 1 GHz. The waveform measured by the sensor was almost the same as the applied waveform.

5. Conclusion

The new broadband optical E-filed sensor has been developed to operate more than 10 GHz. The experiment indicates that the element length is not a unique parameter to design the optical E-filed sensor. The investigation shows the transit time effect is also important factor to design the sensor operating above several GHz. The calculation result shows the electrode length should be less than 1 mm for the sensor to operate more than 10 GHz.

An isotropic sensor has been fabricated using three optical E-filed sensors, which was designed considering the transit time effect. The minimum detective electric filed strength of the sensor is 22 mV/m and this is 100 times that of a commercial E-filed sensor. The deviation of sensitivity for direction is within ±1 dB when the sensitivity of the each sensor is compensated. The sensitivity of the sensor is within ±3 dB up to 5 GHz and within ±5 dB up to 10 GHz. The frequency response is almost agreed to the calculated results. It has been confirmed that frequency characteristic can be designed accurately by considering transit time effect of the optical wave. The experiments, which apply the electromagnetic pulse, indicate the sensor is useful to measure the very short electromagnetic pulse.

In future work, we should study the influence of sensor case.

References

[1] IEC/TC77 IEC61000-4-3.
[2] CISPR/A/241/FDIS
[3] CISPR/G/176/FDIS
[4] Y. Maeda, K. Takaya, and N. Kuwabara, "Requirements for controlling coverage of 2.4-GHz-band wireless LANs by using partitions with absorbing board," IEICE Trans. Commun., vol. E83-B, no. 3, pp.525-531, March 2000.
[5] H.B. Berger, V. Kumara, and K. Matloubi, "A broad-band E-field sensing system," Proc. 1988 IEEE Symp. Electromagn. Compat., pp.383-389, Seattle, Aug. 1988.
[6] N. Kuwabara and R. Kobayashi, "Development of Electric Field Sensor using Mach-Zehnder Interferometer," Proc. 11th International Zurich Symp. on EMC, pp.489-494 , Switzerland, 1995.
[7] M. Schwerdt, J. Berger, and K. Petermann, "E-field measurements in the near-field of transmitting antennas using an integrated electro-optical sensor," IEEE. International Symp. on EMC, pp.474-476, Santa Clara, 1996.
[8] F. Gassmann and M. Mailand, "A 9 channel photonic isotropic electric and magnetic field sensor with subnanosecond rise time," Proc. 12th International Zurich Symp. on EMC, pp.217-221, Switzerland, 1997.
[9] P. Bienkowski and H. Trzaska, "Frequency limitations in photonic EMF probes," Proc. 12th International Zurich Symp. on EMC, pp.603-606, Switzerland, 1997.
[10] M. Schwerdt, J. Berger, and K. Petermann, "An integrated optical E-field sensor using a reflection scheme," Proc. 12th International Zurich Symp. on EMC, pp.597-602, Switzerland, 1997.
[11] K. Tajima, N. Kuwabara, R. Kobayashi, and M. Tokuda, "Evaluation of electric field sensor with very small elements using Mach-Zehnder interferometer," IEICE Trans., vol.79-B-áU, no.11, pp.744-753, Nov. 1996.
[12] M. Izutsu, Y. Yamane, and T. Sueta, "Broad-band traveling wave modulator using a $LiNbO_3$ waveguide," IEEE J. Quantum Electron., vol.QE-13, no.4, pp.287-290, 1977.
[13] K. Kubota, J. Noda, and O. Mikami, " Traveling wave optical modulator using a directional coupler $LiNbO_3$ waveguide," IEEE J. Quantum Electron., vol.QE-16, no.7, pp.754-760, 1980.
[14] K. Tajima, R. Kobayashi, N. Kuwabara, and M. Tokuda, "Frequency bandwidth improvement of electric field sensor using optical modulator by resistively loaded element," Trans. IEE of Japan, vol.117-A, no.5, pp.515-522, 1997.
[15] M. Kanda and L.D. Driver, "An isotropic electric-field probe with tapered resistive dipoles for broadband use,100 kHz to 18 GHz," IEEE Trans. Microwave Theory & Tech., vol.MTT-35, no.2, pp.124-130, Feb. 1987.

Kimihiro Tajima received the BE and ME degrees in Electronic Engineering from Kumamoto University, Kumamoto, Japan in 1986 and 1989 respectively. He entered NTT Telecommunication Networks Laboratories. He has been engaged in the studies on the optical measuring methods for EMC. In 1991–1993, he was engaged in technical supports for EMC troubleshooting in field at NTT Technical Assistance and Support Center. He was a Senior Research Engineer of NTT Lifestyle and Environmental Technology Laboratories and researched mobile communication systems using infrared rays until Oct. in 2000. Currently, He is a manager in NTT Service Integration Laboratories. Mr.Tajima is a member of IEEE.

Ryuichi Kobayashi received the BE and ME degrees in Communication Engineering from University of Electro-Communications, Tokyo, Japan in 1991 and 1993 respectively. He entered NTT Telecommunication Networks Laboratories. He has been engaged in research and development of optical measurement technique for EMC. Currently, he is a Chief engineer of NTT Technical Assistance and Support Center. Mr.Kobayashi is a member of IEEE and URSI.

Nobuo Kuwabara received the BE and ME degrees in Electrical Engineering from Shizuoka University, Shizuoka, Japan in 1974 and 1976 respectively, and the Dr. Eng. degree from Shizuoka University in 1992. Since joining NTT in 1977, he has been engaged in research on the electromagnetic compatibility and protection of telecommunication systems. He is currently a Professor in Department of Electrical Engineering, Kyushu Institute of Technology. Prof. Kuwabara is a member of IEEE.

Masamitsu Tokuda received the BE and ME degrees in Electronic Engineering from Hokkaido University, Hokkaido, Japan in 1967 and 1969 respectively. He joined the Electrical Communication Research Laboratory and he has been engaged in research on transmission measurement of optical cables and EMC for telecommunication networks. He is currently a Professor in Faculty of Electrocommunication Engineering of Musashi Institute of Technology. Prof. Tokuda is a member of IEEE.